



# Polyelectrolyte mediated nano hybrid particle as a nano-sensor with outstandingly amplified specificity and sensitivity for enzyme free estimation of cholesterol



Mazhar Chebl<sup>a</sup>, Zeinab Moussa<sup>a</sup>, Markus Peurla<sup>b</sup>, Digambara Patra<sup>a,\*</sup>

<sup>a</sup> Department of Chemistry, American University of Beirut, Beirut, Lebanon

<sup>b</sup> Laboratory of Electron Microscopy, University of Turku, Turku, Finland

## ARTICLE INFO

### Keywords:

COL  
Curcumin  
Silica Nanoparticles  
Cholesterol  
Biosensing

## ABSTRACT

As a proof of concept, here it is established that curcumin integrated chitosan oligosaccharide lactate (COL) self-assembles on silica nanoparticle surface to form nano hybrid particles (NHPs). These NHPs have size in the ranges of 25–35 nm with silica nanoparticle as its core and curcumin-COL as outer layer having thickness of 4–8 nm. The fluorescence intensity of these NHPs are found to be quenched and emission maximum is ~50 nm red shifted compared to free curcumin implying inner filter effect and/or homo-FRET between curcumin molecules present on the surface of individual nano hybrid particle. Although fluorescence of free curcumin is remarkably quenched by  $\text{Hg}^{2+}/\text{Cu}^{2+}$  ions due to chelation through keto-enol form, the fluorescence of NHPs is unaffected by  $\text{Hg}^{2+}/\text{Cu}^{2+}$  ion that boosts analytical selectivity. The fluorescence intensity is outstandingly enhanced in the presence of cholesterol but is not influenced by ascorbic acid, uric acid, glucose, albumin, lipid and other potential interfering substances that either obstruct during enzymatic reaction or affect fluorescence of free curcumin. Thus, NHPs outstandingly improve analytical specificity, selectivity and sensitivity during cholesterol estimation compared to free curcumin. The interaction between cholesterol and NHPs is found to be a combination of ground state electrostatic interaction through the free hydroxyl group of cholesterol along with hydrophobic interaction between NHPs and cholesterol and excited state interaction. The proposed cholesterol biosensor illustrates a wider linear dynamic range, 0.002–10  $\text{mmol L}^{-1}$ , (upper limit is due to lack of solubility of cholesterol) needed for biomedical application and better than reported values during enzymatic reaction. In addition, the NHPs are found to be photo-stable potentially making it suitable for simple, quick and cost-effective cholesterol estimation and opening an alternative approach other than enzymatic reaction using nano hybrid structure to tune analytical specificity, selectivity and sensitivity of probe molecule.

## 1. Introduction

Smart polymers having responsive properties have received various interests [1]. Such materials are getting widely utilized in nanoscience and nanotechnology towards sensor designing since two decades [2]. Thus, this field has witnessed fast development and advancement during this period. All types of nanoparticles can be incorporated into different polymeric materials to develop nanoscale sensors. Such nanosensors can be applied in both gas and liquid media analysis [2]; therefore, there are tremendous demands for utilizing nanomaterials as biosensing probes. Based on the hybridization between a target and its complementary probe, various electrochemical and optical methods have been successfully achieved using smart polymers [3]. Water-soluble polymers play crucial role for their applicability in

stabilizing nanoparticles, drug delivery, tissue engineering, bioelectronics, biosensing etc [4]. Smart polymers that are non-toxic, biologically compatible and chemically versatile are of special interest to create a plethora of formulations and scaffolds for utilization in health care [5]. Chitosan is one such special polymer which self-assemble by changing the pH [6], thus, it has a distinctive combination of properties [7]. Moreover, chitosan is biodegradable, biocompatible and bioactive polymer. Therefore, it has gained a wide range of applications in biomedical use [8]. Chemically chitosan is a polysaccharide and obtained by partial chitin N-deacetylation under alkaline conditions. It is a linear random distribution of N-acetylglucosamine and glucosamine units, and more water-soluble than chitin due to the presence of the protonated amine group. Chitosan oligosaccharide lactate (COL) (see Fig. S1A) is a minor modification form of chitosan, having a

\* Corresponding author.

E-mail address: [dp03@aub.edu.lb](mailto:dp03@aub.edu.lb) (D. Patra).

<http://dx.doi.org/10.1016/j.talanta.2017.03.070>

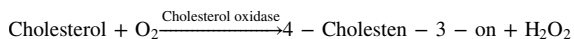
Received 30 January 2017; Received in revised form 22 March 2017; Accepted 23 March 2017

Available online 25 March 2017

0039-9140/ © 2017 Elsevier B.V. All rights reserved.

shorter chain and lactate as a counter ion, to enhance further water solubility. Below its pKa, COL exists in polyelectrolyte form due to positively charged amine groups, which can interact with anionic or neutral group by electrostatic and/or hydrophobic interaction between polymer backbone and the charged/hydrophobic entity of interacting molecule.

Cholesterol is a biomolecule and part of the sterol family characterized by a four-ring structure and a hydroxyl group at the 3-position of ring A, which makes the polar part of the molecule. Cholesterol is found mainly in the animal cell membrane [9] where its presence contributes in decreasing the membrane fluidity [10] and reduces its permeability for polar molecules due to its lateral ordering of neighboring lipids [11]. Cholesterol can be directly synthesized from acetyl-CoA through the mevalonate pathway [12] or it can be imported through dietary [13]. The presence of cholesterol in blood at high concentration increases the risk of cardiac and brain vascular diseases [14]. In addition to other conditions, Alzheimer and type-2 diabetes are linked to cholesterol [15]. Moreover, few studies have suggested an increase in risk of cancer related to a low level of serum cholesterol [16]. Therefore, determination of cholesterol by rapid, cost-effective and reliable methods is considered very crucial for clinical diagnosis. A total level of 200 mg dl<sup>-1</sup> (5.18 mmol L<sup>-1</sup>) of cholesterol is considered best as reported by the National Institute of Health, and according to the American Heart Association [17]; nonetheless, patient with high cholesterol level exhibits no symptoms, therefore, it necessitates periodical clinical test. Gravimetric, colorimetric and chromatographic techniques have been developed for cholesterol determination in blood and different food samples, but these methods are expensive and nonspecific. Few of them like GC, requires cholesterol derivatization [18]. Electrochemical-based biosensor for cholesterol determination is getting recently popular by immobilizing cholesterol oxidase (and cholesterol esterase for total cholesterol determination) on the surface of the electrode [19]. Indirect electrochemical method is based on following oxygen reduction current [20] with an O<sub>2</sub> electrode or following either the reduction or the oxidation current of the generated hydrogen peroxide [21] as below.



In addition to the indirect detection method, direct electron transfer between the immobilized cholesterol oxidase and the electrode surface has been a subject of study using a carbon modified composite electrodes with an enhanced electron transfer between the ChOx(FAD) deeply buried electroactive species and the surface of the electrode surface [22]. However, these enzymes based electrochemical biosensors require a development step to adapt and enhance the surface of the electrode followed by cholesterol oxidase immobilization. A mediator is generally used to lower the detection limit, and the presence of interferences such as ascorbic and uric acid that can be easily oxidized in the same range of H<sub>2</sub>O<sub>2</sub> oxidation potential (+0.6 V). In addition, other constraints include optimum working temperature and pH of the enzyme used. Alternatively, fluorescence based methods have been tried using nanoparticles in combination of enzymatic reaction [23]. Kim et al have reported an enzyme (ChOx) modified CdSe/ZnS quantum dots for cholesterol sensing based on the change in quantum dot fluorescence [24]. Since fluorescence methods using enzymatic reaction is also based on indirect detection of hydrogen peroxide, these methods also suffer due to interference from other substances.

On the other hand, there are little report on selective cholesterol sensing using fluorescence probe without enzymatic reaction [25]. This is because of the fact that many fluorescent molecules used directly as probe have poor selectivity and poor stability for the target analytical species. Analytical specificity in fluorescence probe based method has long been an intriguing topic that plays a crucial role during estimation for targeted biomedical species. Although enzymatic reaction, base stacking (aptamers) and antigen-antibody linkers are few possibilities,

each of these possibilities has their own limitations and gets influence by foreign interference. The other way of addressing such problem could be tuning the probe molecule by using emerging nanotechnology, such as nano hybrid structures. Curcumin, which is bis (4-hydroxy -3-methoxyphenyl) -1, 6- diene- 3, 5- dione, is a food spices and has shown effective therapeutic properties [26]. Recently curcumin as a molecular probe to study micelle, liposomes, and heterogeneous systems is widely getting realized [27]. It is also being used for fluorescence nano-sensing [28] and is useful for synthesis of nanoparticles along with polymer matrix [29]. Curcumin as a fluorescence probe for estimating biological analyte has a great potential. Moreover, few studies have shown positive impact of curcumin on blood cholesterol level [30]. In this manuscript, as a proof of concept we propose that COL along with curcumin can be integrated with negatively charged silica nanoparticles to form nano hybrid particles (NHPs), which can be used as a novel analytical technique for cholesterol sensing without enzymatic reaction. The advantages of this method are: (i) synthetic procedure is easy; (ii) materials are stable and robust; (iii) it is highly selective for cholesterol and superior than enzymatic estimation; and, (iv) it has a wider linear dynamic range compared with reported values.

## 2. Material and method

### 2.1. Materials

Curcumin, COL, cholesterol, ascorbic acid, Silica LUDOX<sup>®</sup> HS-40 Colloidal Silica, 6-O-palmitoyl-L-ascorbic, bovine serum albumin, vitamin E, ascorbic acid, uric acid, urea, glucose, palmitic acid, methyl nonadecanoate, oleic acid, and metal ions such as calcium chloride, magnesium sulfate, zinc nitrate, nickel nitrate, sodium fluoride, lead nitrate, iron (II) sulfate, mercury nitrate, and copper sulfate were obtained from Sigma-Aldrich. All the solvents used were from Sigma-Aldrich.

### 2.2. NHPs preparation

A stock solution of 1 mg mL<sup>-1</sup> chitosan oligosaccharide lactate dissolved in 1% acetic acid was prepared, similarly 16 mmol L<sup>-1</sup> of curcumin solution in methanol was made. 20 μL of curcumin stock solution was added to 2 mL chitosan oligosaccharide lactate stock solution and was kept stirring for couple of hours. After that, 120 μL of the LUDOX silica was added drop wise under continuous stirring, then the whole solution was kept stirred overnight. The formed capsules were left to precipitate, the supernatant solution was discarded and the capsules were dispersed in 2 mL of distilled water to be used later on.

### 2.3. Sample preparation

Different stock solutions, each containing an analyte at a concentration of 6 mmol L<sup>-1</sup> dissolved in double distilled water, were prepared. However, for stock solutions, cholesterol, 6-O-palmitoyl-L-ascorbic acid, vitamin E, methyl ester (methyl nonadecanoate) and palmitic acid were dissolved in methanol. In order to assert the effect of methanol on the fluorescence of the nano hybrid particles, different amounts of methanol were used in a cholesterol free medium. For the fluorescence measurement, 100 μL of the dispersed NHPs were added to 2900 μL of water followed by 50 μL of the prepared analyte solution. For the establishment of cholesterol calibration curve, the 100 μL NHPs solution was dispersed in 2500 μL of distilled water, followed by 400 μL of cholesterol dissolved in methanol at the desired concentration.

### 2.4. Instrumentation

Transmission electron microscopy (TEM) measurement was carried

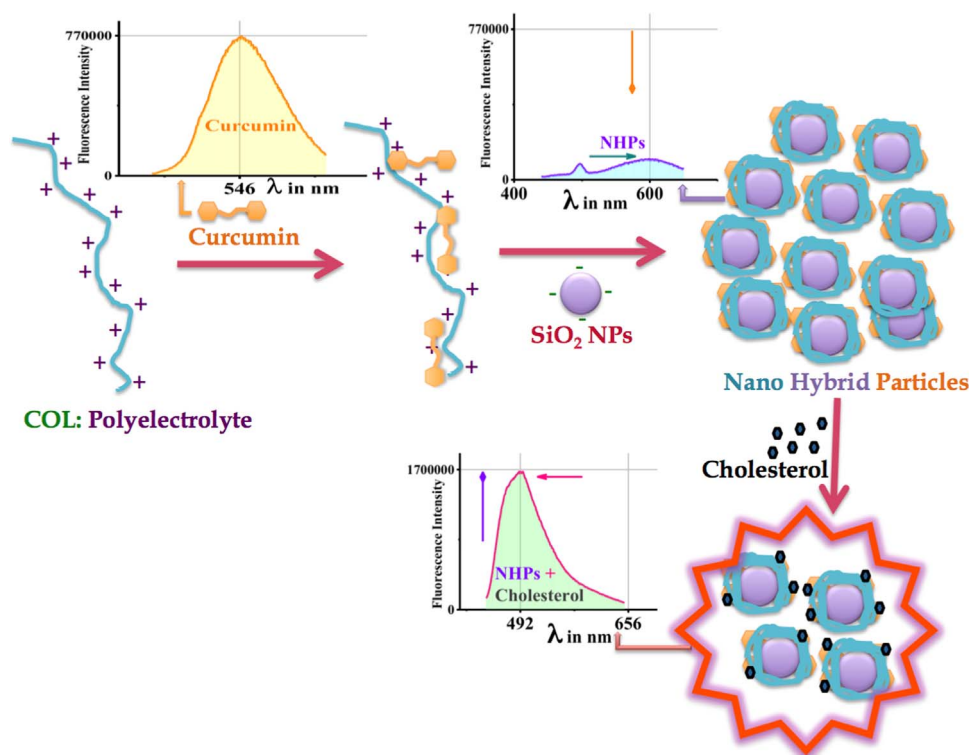


**Fig. 1.** Illustration of nano hybrid particles formation in the presence of polyelectrolyte (COL), curcumin, silica nanoparticles ( $\text{SiO}_2$  NPs) and enhancement in fluorescence in the presence of cholesterol.

out with a JEOL JEM-1400Plus, operating at 120 kV. TEM samples were prepared by casting a drop of the NHPs suspension onto copper grids covered with carbon films. Scanning electron microscopy (SEM) analysis was done using Tescan, Vega 3 LMU with Oxford Edx detector (Inca XmaW20) SEM, where 3 mg of the NC were dissolved in 5 mL of de-ionized water, and few drops of the NHPs suspension were mounted on an aluminum stub, coated with carbon adhesive. After being dried the sample was ready for the SEM analyses. XRD data was collected using a Bruker D8 advance X-ray diffractometer (Bruker AXS GmbH, Karlsruhe, Germany) at 40 kV, 40 mA (1600 W) using Cu K $\alpha$  radiation ( $\lambda=1.5418 \text{ \AA}$ ), with a 1.2 mm primary beam slit and 2.0 mm detector slit. The X-ray scans were carried out for  $2\theta$  between 5 and  $70^\circ$  at  $0.02^\circ$  increments.

### 2.5. Spectroscopic method

FT-IR spectra were recorded using a Thermo Scientific Nicolet iS5 FT-IR Spectrophotometer using KBr palate. The absorption spectra were recorded using a JASCOV-570 UV-VIS-NIR spectrophotometer at room temperature. The steady-state fluorescence spectra (excitation and emission) were recorded at room temperature using Jobin-Yvon-Horiba Fluorolog III fluorometer and the FluorEssence program where the excitation and emission slits width were 5 nm. The source of excitation was a 100 W Xenon lamp, and the used detector was R-928 operating at a voltage of 950 V. The fluorescence lifetime measurements were done using the same instrument except a pulsed diode laser of excitation wavelength 405 nm was used for excitation. Instrumental response (prompt) for lifetime measurement was carried out using colloidal non-fluorescent particles. The decay data were analyzed using Data Analysis Software.

## 3. Results and discussion

### 3.1. Preparation of nano hybrid particles

When suspended in water and imaged on continuous formvar film TEM image of COL showed a leaf-like pattern in microscopic scale (Fig. S1B and also inset), however, in nanoscopic level there were no regular pattern (Fig. S1C). Bright field image (Fig. S1D) and corresponding dark field image (not shown) of COL illustrated similar pattern and the diffraction pattern (inset of Fig. S1D) of COL suggests crystalline nature of the materials. At low concentration, COL remains in monomeric form due to no major interaction between the acetylated unit and the surrounding. Chitosan has a pKa value in the range 5.5–6.5 [31] and COL in acidic solution (at pH 2.8) forms polyelectrolyte (see Fig. S2A) due to protonation of the amine group. When curcumin was mixed with COL, fluorescence intensity of curcumin was quenched without affecting the emission maximum (Fig. S2B) by monomeric form (below the critical aggregation concentration,  $cac$ ) of COL, however, COL in aggregated form (above the  $cac$ ) recovered the loss in fluorescence intensity of curcumin and further increase in COL concentration enhanced the fluorescence intensity along with a blue shift in the emission maximum of curcumin (see Fig. S2B). This suggests interaction of curcumin with COL in polyelectrolyte form is very strong. The fluorescence intensity variation of curcumin with COL concentration demonstrated in Fig. S2C could able to locate  $cac$  of COL, at  $\sim 5 \mu\text{mol L}^{-1}$ . This result is similar to that obtained for curcumin in neutral pH condition earlier [32]. The partition of curcumin into polyelectrolyte form of COL (in acidic condition) was evaluated above  $cac$  using the following equation [33]:

$$\frac{1}{F} = \frac{55.6}{P_{COL/Water} F_0} \frac{1}{[COL]} + \frac{1}{F_0}$$

where  $F_0$  is the fluorescence intensity when curcumin is in the COL aggregates, and 55.6 mol/L represents water concentration in a dilute medium. A linear plot of  $1/F$  versus  $1/[COL]$  (see Fig. S2D) led to

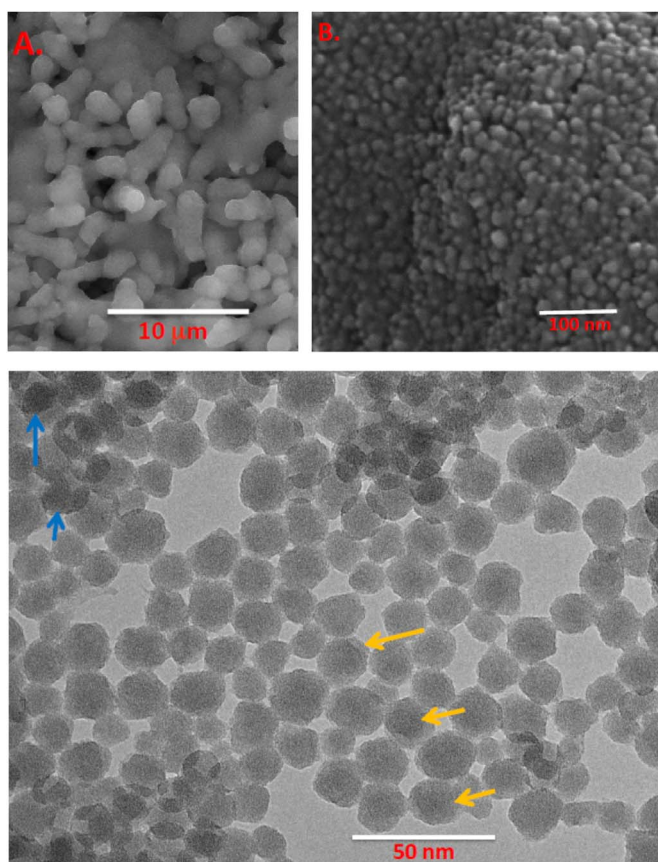


**Fig. 2.** SEM images of NHPs in aggregated form (A) and at higher resolution showing individual NHPs (B); (C) TEM images of NHPs, the darker particle inside and a fainter outer layer can be seen in yellow arrows marked images, however, the darker contrast due to overlapping of two or more particles can also be seen in blue arrows marked images. (For interpretation of the references to color in this figure legend, the reader is referred to the web version of this article.)

estimate partition coefficient ( $P_{\text{COL}/\text{Water}}$ ) from the intercept and slope. Interestingly, partition of curcumin into COL could be amazingly enhanced in acidic condition ( $P_{\text{COL}/\text{Water}} = 7.75 \times 10^6$ ) compared to measured earlier in neutral condition ( $P_{\text{COL}/\text{Water}} = 1.23 \times 10^{-3}$ ) [32]. This could be due to polyelectrolyte form of COL at pH 2.8, which is similar to association of curcumin with another polyelectrolyte such as poly (allylamine hydrochloride) [34] and poly ( $\alpha$ -lysines) [35]. Therefore, for efficient encapsulation of curcumin in COL phase, acidic medium (below pKa) serves the best.

To enhance stability and partition of curcumin into COL, we prepared NHPs by self-assembly method. The self-assembly of COL was achieved using silica nanoparticles ( $\text{SiO}_2$  NPs). COL in polyelectrolyte form (in the presence of 1% acetic acid) was mixed with curcumin under stirring for couple of hours. To this aggregated solution, 120  $\mu\text{L}$  of silica nanoparticles of size  $\sim 20$ – $24$  nm at pH  $\sim 9.8$  was added drop wise. The obtained cloudy solution was kept for overnight. When less than 100  $\mu\text{L}$   $\text{SiO}_2$  NPs was used, there was no formation of cloudy solution, thus, concentration of  $\text{SiO}_2$  NPs plays an important role during formation of NHPs. The cloudy solution was centrifuged and washed for three times in deionized water to discard unreacted COL, curcumin and  $\text{SiO}_2$  NPs. Finally, hybrid particles were dispersed in doubly distilled water for further characterization and investigation. Due to their overall net negatively charges,  $\text{SiO}_2$  NPs assist assembly of positively charged COL (in polyelectrolyte form) conjugated with curcumin on its surfaces to form spherical NHPs as illustrated in Fig. 1.

The size and shape of these obtained NHPs were characterized by SEM. SEM image depicted in Fig. 2A indicates shape of these particles

is spherical, few elongated particles were also obtained. Sizes of these particles varied in the ranges 1–3  $\mu\text{m}$ . Earlier we have observed that polyamines cross links in the presence of multivalent anions such as phosphate [34], citrate [36] etc. which subsequently facilitates aggregation of nanoparticles to form spherical microcapsules in the range of 0.5–4  $\mu\text{m}$  with a thickness of 100–250 nm of silica nanoparticles. Interestingly, higher magnification, shown in Fig. 2B, establishes that in the present case these large particles are aggregated form of smaller and spherical nanoparticles with diameters in the ranges  $\sim 25$ – $35$  nm, which is different from nano-/micro-capsules obtained earlier [28,34–36].

This could be possible in two different scenarios. First scenario could be when COL acts as an outer layer to encapsulate aggregated  $\text{SiO}_2$  NPs altogether, which can form the core of the structure similar to earlier observation in the presence of salt [28,34–36]. However, in this case repulsion from negatively charged  $\text{SiO}_2$  NP may not encourage this scenario. The second scenario is that COL self-assembles on individual  $\text{SiO}_2$  NP surface to form spherical nano hybrid particles, which congregate in aqueous medium to form large structures due to hydrophobic interaction. To understand this, these particles were diluted and sonicated for few seconds and TEM images were taken. The TEM images shown in Fig. 2C indicate spherical particles of diameter 25–35 nm with a dark core representing  $\text{SiO}_2$  NPs and a lighter layer of thickness 4–8 nm over it for COL and curcumin, which proves that the smaller particles are indeed NHPs made up of  $\text{SiO}_2$  NP, COL and curcumin. The role of curcumin during self-assembly of COL on  $\text{SiO}_2$  NP surface was studied. As shown in Fig. S3, NHPs were obtained in the absence of curcumin, thus, curcumin did not influence the self-assembly process of COL.

### 3.2. Characterization of NHPs

FT-IR spectra of NHPs, curcumin, COL and mixture of curcumin and COL are demonstrated in Fig. 3A.  $\text{SiO}_2$  NPs (spectrum not shown) showed an absorption band at  $\sim 3482$   $\text{cm}^{-1}$  due to  $-\text{OH}$  stretching that shifted to  $3415$   $\text{cm}^{-1}$  after binding, in addition to absorbance bands at  $\sim 1637$ , 1108, 973, 798 and  $470$   $\text{cm}^{-1}$  that are the fingerprints of  $\text{SiO}_2$  vibration and stretching. The FT-IR spectrum of NHPs is similar to that of silica with a shift to  $802$  and  $472$   $\text{cm}^{-1}$  of  $\text{Si}-\text{O}-\text{Si}$  vibrational peaks and the appearance of a small peak at  $2963$   $\text{cm}^{-1}$  relative to  $\text{C}-\text{H}$  stretching vibration. Note that Lai et al. [37] have reported an increase in the sharpness of the peak at  $1108$   $\text{cm}^{-1}$  as its concentration increases, therefore, upon NHPs formation this peak got broadened due to the presence of COL. The vibration of the free hydroxyl groups of COL was found at  $\sim 3620$ – $3650$   $\text{cm}^{-1}$  and that of phenolic  $\text{O}-\text{H}$  vibration of curcumin was obtained at  $\sim 3510$   $\text{cm}^{-1}$ . In the mixture of COL and curcumin rather a band was located at  $\sim 3315$   $\text{cm}^{-1}$  instead of peak for phenolic  $\text{O}-\text{H}$  of curcumin or free  $\text{O}-\text{H}$  of COL. In NHPs two peaks at  $\sim 3425$   $\text{cm}^{-1}$  and  $3650$   $\text{cm}^{-1}$  were found suggesting the interaction between COL and curcumin is different in NHPs compared to in the mixture of COL and curcumin. The peak at  $\sim 2973$   $\text{cm}^{-1}$  because of enolic  $\text{O}-\text{H}$  vibration (note that  $\text{sp}^3$   $\text{C}-\text{H}$  stretching also has the vibration in the same region, but often in curcumin case band in this region has been shown to be for  $\text{O}-\text{H}$  vibration) in curcumin could be prominently identified in NHPs. The band at  $\sim 2900$   $\text{cm}^{-1}$  found in COL and COL-curcumin mixture could also be detected in NHPs. In COL, the vibrational bands due to amide groups at  $\sim 1560$   $\text{cm}^{-1}$  and  $1404$   $\text{cm}^{-1}$  were identified, similarly bands at  $\sim 1627$  and  $\sim 1602$   $\text{cm}^{-1}$  for  $\alpha$ - $\beta$  unsaturated ketone and enol form of curcumin were clearly established. In the mixture, the amide groups of COL and ketone and enol form of curcumin were obtained to be in the same region, however, in NHPs a band at  $\sim 1656$   $\text{cm}^{-1}$  was found indicating electrostatic and/or strong hydrogen bond types of interaction between  $\text{SiO}_2$  NP, COL and curcumin. Fig. 3B shows curcumin XRD pattern exhibiting several characteristic diffraction peaks ranging from  $2\theta = 5$ – $30^\circ$ , whereas NHPs loaded with curcumin showed only one broad peak

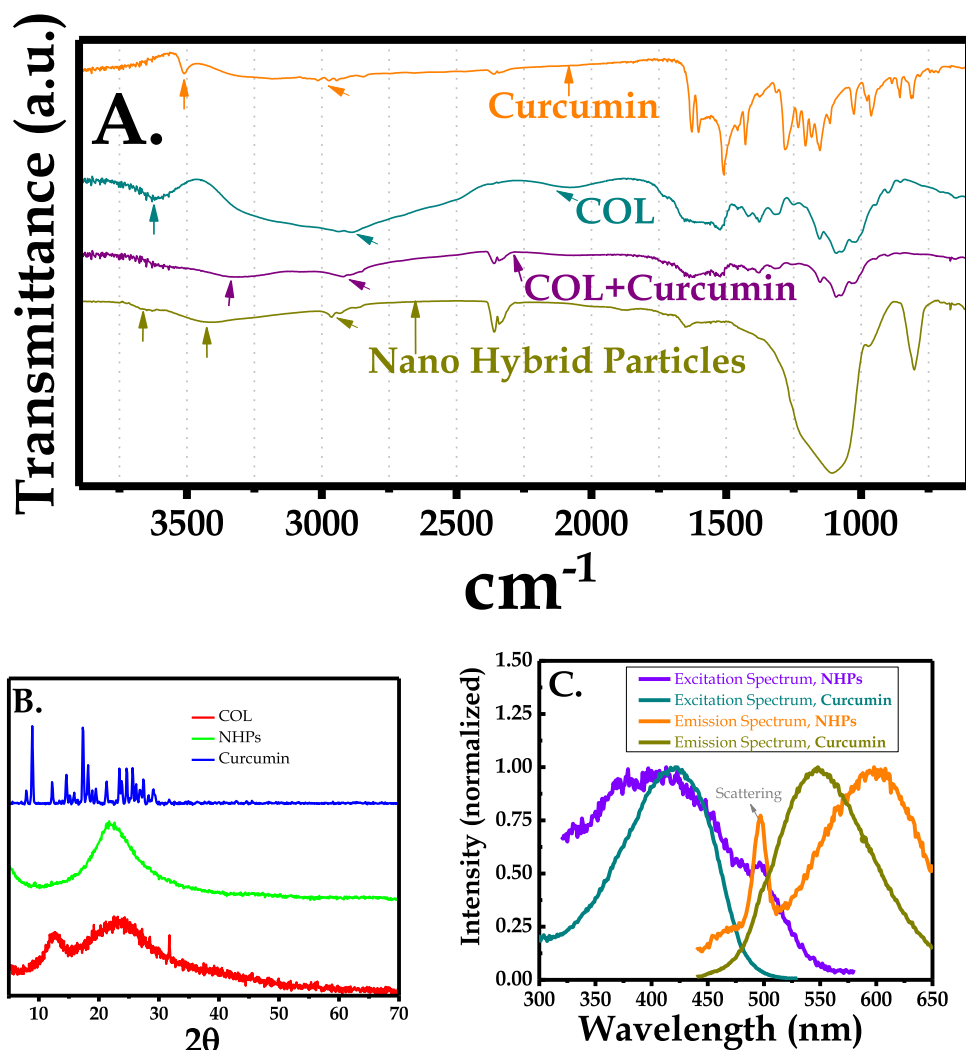


**Fig. 3.** (A) FT-IR spectra of NHPs, COL and Curcumin; (B) XRD pattern of NHPs, COL and Curcumin; (C) Fluorescence excitation and emission of NHPs and curcumin in doubly distilled water, the fluorescence intensity has been normalized with respect to intensity at the peak position.

with a maximum at  $2\theta = 21.7^\circ$  due to the amorphous nature of silica with an alteration of all the peaks of curcumin and COL. A similar observation was reported in literature [38,39], arguing that curcumin loses its crystallinity after forming a complex with the  $\text{SiO}_2$  NP-COL matrix.

### 3.3. Optical properties of NHPs

Curcumin absorbs at around  $\sim 425$  nm in buffer solution due to strong  $\pi(\text{HOMO}) \rightarrow \pi^*(\text{LUMO})$  transition, which masks the weak electronic dipole forbidden  $n \rightarrow \pi^*$  band [40]. Curcumin loaded NHPs has a continuous absorption that is higher at shorter wavelengths, which is largely due to strong scattering of nanoparticles, but the absorption band of curcumin at  $\sim 425$  nm was identified in NHPs (not shown). Excitation spectrum of curcumin showed a similar peak like absorption spectrum, which is in agreement with the theoretically predicted value for curcumin in enol form [41], no peak at around 355 nm was found for NHPs signifying that curcumin is predominately in enol form in NHPs. However, the excitation spectrum of NHPs was found to be broad with a minor blue shift in excitation maximum (see Fig. 3C). The fluorescence emission spectrum of NHPs at excitation wavelength 425 nm was found to be broad and similar to obtained for free curcumin, but the emission maximum of NHPs red shifted remarkably,  $\sim 50$  nm, compared to free curcumin. The fluorescence intensity of NHPs was also significantly found to be quenched in NHPs

compared to free curcumin in buffer solution. When curcumin was mixed with silica nanoparticles [28], the fluorescence emission spectrum showed a large blue shift from  $\sim 550$  nm in water to around 495 nm, therefore, the obtained red shift in NHPs is not due to direct interaction between curcumin and  $\text{SiO}_2$  NP. Earlier it is also found that while interacting with polyelectrolyte such as PAH [34] and PLL [35], the fluorescence spectrum of curcumin shifts towards shorter wavelength range. While interacting with hydrophobic pockets like in micelle or liposomes, curcumin also shows a blue shift peaked at  $\sim 492$ – $510$  nm [27], whereas diketone form of curcumin has an emission maximum in lower wavelength range [34]. Thus, the large red shift observed for NHPs excludes any kind of hydrophobic association or due to keto form of curcumin. In addition, the absorption maximum did not demonstrate a major shift suggesting there is no ground state aggregation that could lower the energy gap between  $\pi(\text{HOMO}) \rightarrow \pi^*(\text{LUMO})$  transition to shift the absorption/emission in longer wavelength. Thus, the observed red shift along with reduction in fluorescence intensity could be due to intermolecular energy transfer between curcumin molecules i.e. homo-Fluorescence Resonance Energy Transfer (homo-FRET) or inner filter effects of molecules present in individual NHPs [42].

### 3.4. Interference from metal ions

A set of metal ion interferents that are reported to bind with

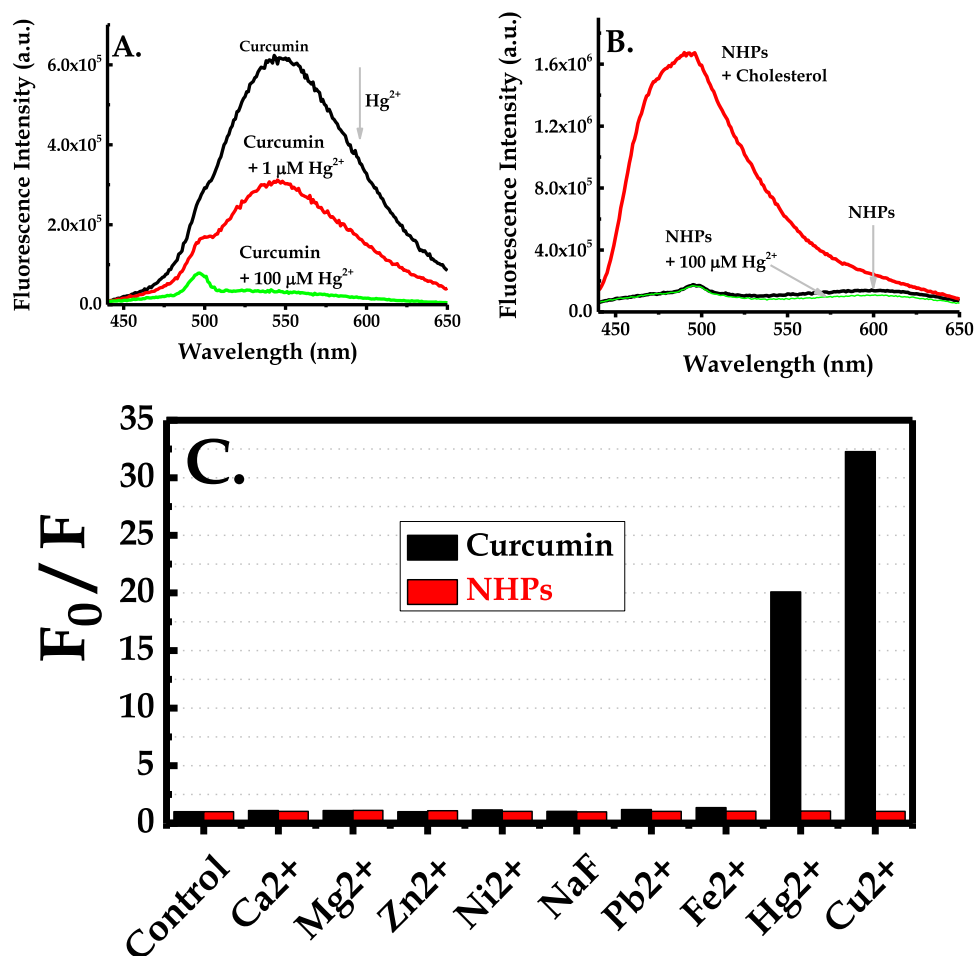


**Fig. 4.** (A) Fluorescence spectra of curcumin in the absence and presence of  $Hg^{2+}$  ion in water; (B) Fluorescence spectra of NHPs in the absence and presence of  $Hg^{2+}$  ion and in the presence of cholesterol in water; (C) Comparison of fluorescence quenching ( $F_0/F$ ) of curcumin and NHPs in the presence of different metal ions. Concentrations of metal ions were fixed at  $100 \mu M$ .

curcumin and affect its emission intensity were prepared and tested against curcumin and the prepared NHPs. Fluorescence intensity of curcumin was highly quenched in the presence of  $Hg^{2+}$  ion without affecting the emission maximum.  $100 \mu mol L^{-1}$  of  $Hg^{2+}$  ion almost quenched all the fluorescence coming out of curcumin (see Fig. 4A). Similar gradual decrease of fluorescence of curcumin by  $Hg^{2+}$  ion in DMSO: water (5:1) mixture has been reported earlier [43]. However, when NHPs was used instead of curcumin, there was almost no effect on fluorescence intensity even at  $100 \mu mol L^{-1}$  of  $Hg^{2+}$  ion as illustrated in Fig. 4B indicating binding of  $Hg^{2+}$  with curcumin is completely blocked in NHPs. Similar results were obtained for  $Cu^{2+}$  ions, although the fluorescence quenching rate of curcumin by  $100 \mu mol L^{-1}$   $Hg^{2+}$  ion was  $\sim 20$  fold whereas by  $100 \mu mol L^{-1}$   $Cu^{2+}$  ion was  $\sim 32$  fold (see Fig. 4C) compared to metal ion free medium. Metal ions like  $Hg^{2+}$  or  $Cu^{2+}$  can make complex with curcumin and it has been proposed that  $Cu^{2+}$  chelates with keto-enol form of curcumin [44]. When fluorescence of NHPs was measured in the presence of as high as  $100 \mu mol L^{-1}$  of  $Cu^{2+}$  ions, there was no appreciable influence on fluorescence intensity of NHPs. The lack of fluorescence quenching of NHPs in the presence of  $Hg^{2+}$  or  $Cu^{2+}$  ions suggests that keto-enol form of curcumin in NHPs is probably not free to chelate with these metal ions due to interaction of keto-enol form with COL-SiO<sub>2</sub> hybrid structures. This experiment further reconfirms hydrogen bond/electrostatic interaction between curcumin and COL/SiO<sub>2</sub> NP in NHPs, which is supported by FT-IR spectra observed earlier. Cholesterol has similarity with the structure of bile salt like cholate and deoxycholate. Cholate/deoxycholate has similar kind of electrostatic (in monomeric

form) and hydrophobic (aggregated form) interaction with curcumin [45]. In addition, preferential complexation of the metal with the amine  $-NH_2$  function of COL can't be ruled out either [46].

### 3.5. Cholesterol estimation

Once interference from metal was ruled out, NHPs were tested for fluorescence sensing of cholesterol. Interestingly, addition of cholesterol remarkably changed the emission maximum and fluorescence intensity of NHPs. A large blue shift of  $> 100$  nm was observed in the fluorescence spectrum of NHPs in the presence of cholesterol with a remarkable increase in fluorescence intensity as demonstrated in Fig. 4B. When free curcumin was used instead of NHPs a similar blue shift of  $\sim 50$  nm and appreciable enhancement in fluorescence intensity were found as shown in Fig. 5A.

The fluorescence maximum and intensity of curcumin is sensitive to hydrophobic pocket [27]. The emission maxima of NHPs and free curcumin were almost identical in the presence of cholesterol centered at  $\sim 493$  nm. This suggests there is a direct interaction between curcumin and cholesterol in NHPs. The spectral shape and emission maximum of curcumin in the presence of cholesterol were similar to observed for curcumin intercalated in liposomes and non-ionic micelles. Intercalation of curcumin due to hydrophobic interaction with liposomes is relatively well established [27]. We suggest similar kind of interaction between curcumin and cholesterol in NHPs. To understand it further, cholesterol was replaced with another hydrophobic molecule, oleic acid and fluorescence spectra of free curcumin and NHPs were

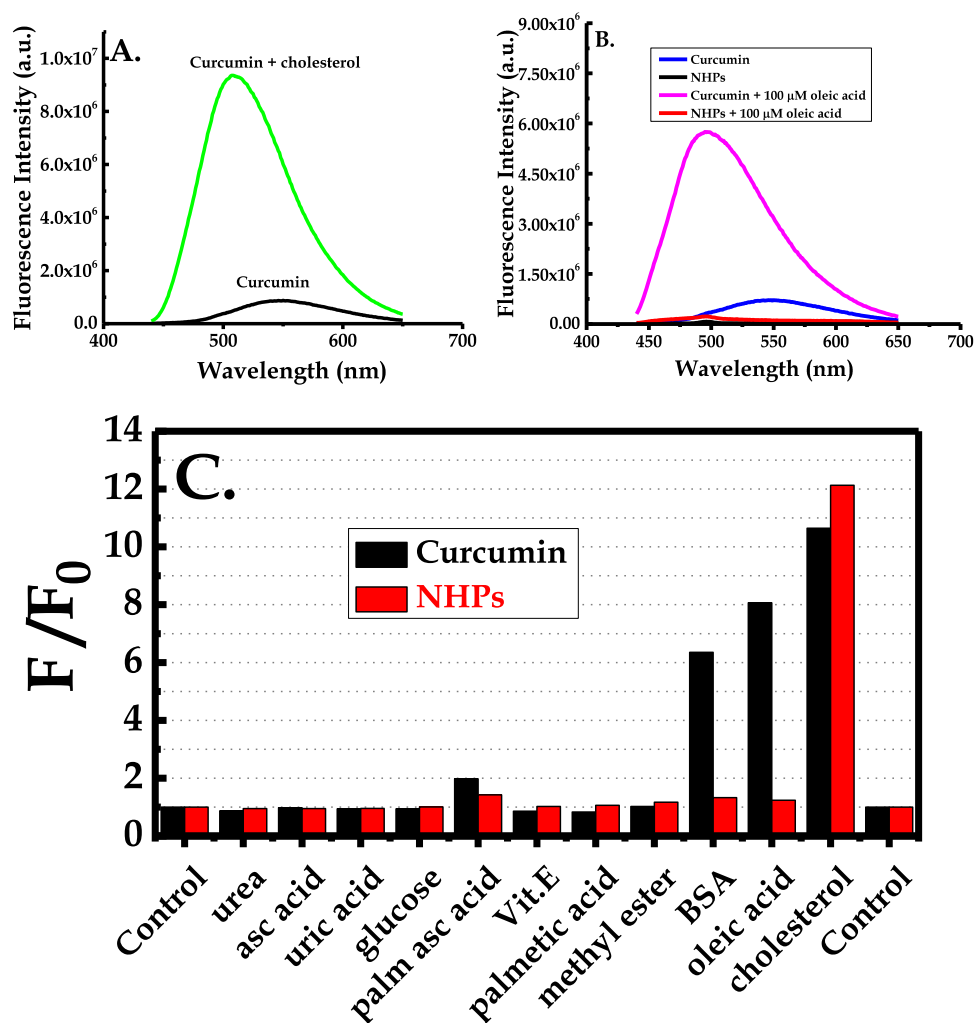


**Fig. 5.** (A) Fluorescence spectra of curcumin in the absence and presence of cholesterol in water; (B) Fluorescence spectra of NHPs and curcumin in the absence and presence of 100 μM oleic acid lipid in water; (C) Comparison of fluorescence enhancement ( $F/F_0$ ) of curcumin and NHPs in the presence of different biomolecules. Concentrations of biomolecules were fixed at 100 μM except for bovine serum albumin (BSA) where 3.3 μM was used.

compared. Interestingly, as depicted in Fig. 5B, the fluorescence intensity of free curcumin increased 8-fold in the presence of 100 μM oleic acid with a large blue shift (~40 nm) in emission maximum whereas there was a nominal change of < 10% in fluorescence intensity of NHPs in the presence of 100 μmol L<sup>-1</sup> oleic acid. Similarly, fluorescence intensity of free curcumin increased 6-fold in the presence of 3.3 μmol L<sup>-1</sup> serum albumin but that of NHPs was negligible (see Fig. 5C). Thus, the interaction of NHPs and cholesterol was special in this case, which is different from that of serum albumin or oleic acid.

### 3.6. Interference study

The potential interference from various substances was tested. Uric acid, ascorbic acid and glucose that interfere in common electrochemical methods for cholesterol quantification, did not affect fluorescence intensity of both NHPs and free curcumin as seen in Fig. 5C. A noteworthy observation is the differential behavior of curcumin in free form and in NHPs in the presence of lipids (palmitic acid, oleic acid), vitamin E and bovine serum albumin. Bovine serum albumin, oleic acid and 6-O-palmitoyl-L-ascorbic acid could interfere during estimation of cholesterol using free curcumin, whereas when NHPs was used interference from these substances could be remarkably minimized apart from suppressing interference from chelating metal ions like Cu<sup>2+</sup>/Hg<sup>2+</sup> ion. There was also no interference from other kinds of possible biochemical (see Fig. 5C) and metal ions (see Fig. 4C). In

addition, the fluorescence enhancement of NHPs was 12 fold higher compared to 10.5 fold for free curcumin in the presence of cholesterol suggesting NHPs enhances both selectivity and sensitivity of cholesterol determination in comparison to free curcumin.

### 3.7. Analytical performance

Comprehending the significance of NHPs for selective and non-enzymatic sensing of cholesterol, the calibration curve for the determination of cholesterol by using NHPs as fluorescence sensing material was established. The fluorescence spectra of NHPs in the presence of different concentrations of cholesterol is shown in Fig. 6A, at very low concentration of cholesterol (~2 μmol L<sup>-1</sup>) the emission maximum of NHPs did not change appreciable but 10 μmol L<sup>-1</sup> of cholesterol was sufficient to completely blue shift the emission maximum to ~493 nm, which was not affected by further increase in cholesterol concentration, even at 10 mmol L<sup>-1</sup> of cholesterol. The fluorescence intensity alteration of NHPs with cholesterol concentration is plotted in Fig. 6B. As can be seen in the plot, in a wide range of concentration range 0–10 mmol L<sup>-1</sup>, the curve showed an exponential growth. The log-log plot illustrated a linear relationship (see inset of Fig. 6B). Chang and Ho [47] have used gold nanocluster assisted fluorescent detection for estimation of cholesterol using enzymatic reaction with a linear dynamic range 2–100 μmol L<sup>-1</sup> where has Li et al. [23] have reported grapheme quantum dots for fluorescence quenching based cholesterol

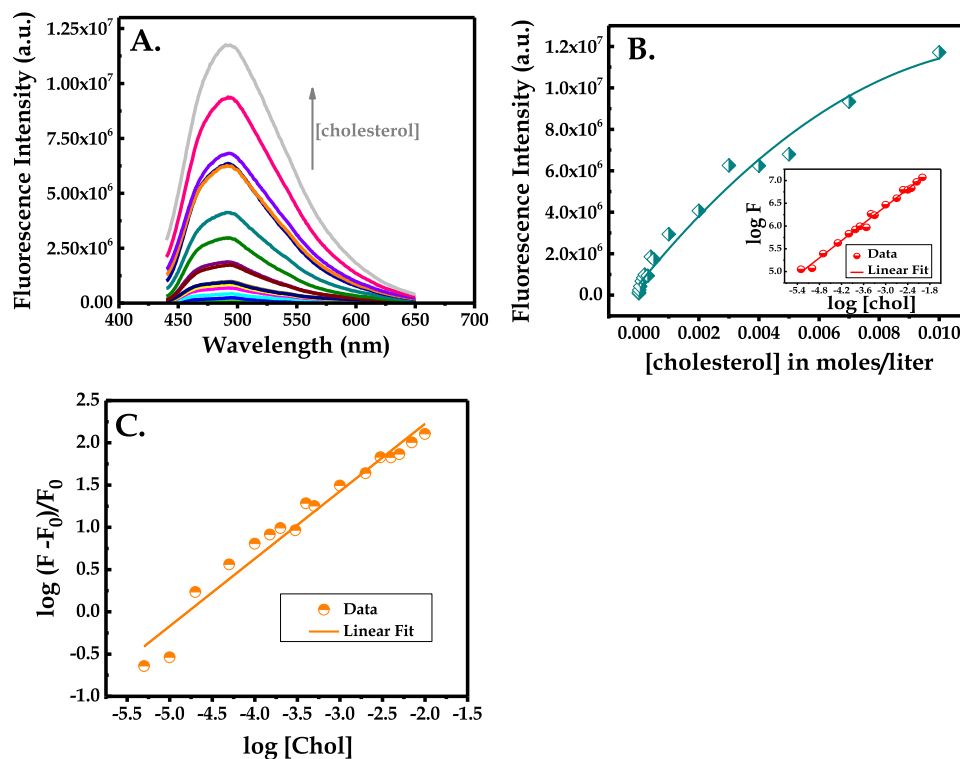


**Fig. 6.** (A) Fluorescence emission spectra of NHPs in the presence of various concentration of cholesterol; (B) Calibration curve for estimation of cholesterol by monitoring fluorescence intensity of NHPs, inset shows log-log plot; (C) Logarithmic plot of  $(F - F_0)/F_0$  vs.  $[\text{cholesterol}]$  (as given in text) while determining association constant of cholesterol with NHPs.

**Table 1**

Comparison of fluorescence and electrochemical sensor performance.

Method	Materials	LOD in $\mu\text{mol L}^{-1}$	Linear Dynamic Ranges in $\text{mmol L}^{-1}$	Reference
Fluorescence	Graphene QDs-ChOx- $\text{H}_2\text{O}_2$	0.08	0.0008–0.01	[23]
Fluorescence	Au-PVP-ChOx- $\text{H}_2\text{O}_2$	1	0.001–0.1	[46]
Fluorescence	Amplex Red-ChOx- $\text{H}_2\text{O}_2$	0.005	0.0005–0.05	[47]
Fluorescence	Au NPs- $\beta$ -CD	0.03	0.0003–0.015	[48]
Fluorescence	Rhodamine B- $\beta$ -CD-FRET	10	0.01–0.12	[49]
Electrochemical	G/Ti(G)-3DNS/CS/ChOx	6	0.05–8.0	[50]
Electrochemical	Pt/TMOS sol-gel/ChOx/p(DB)	–	0.06–3.0	[51]
Electrochemical	Chox/PVF <sup>+</sup> ClO <sup>+</sup> /Pt	–	0.1–5.0	[52]
Electrochemical	ChOx/AgNPs/GCE	180	0.28–3.3	[53]
Electrochemical	MWCNTs-ChOxSiO <sub>2</sub> -chitosan/PB/GCE	1	0.004–0.7	[19]
Electrochemical	ChOx-ChE/AuNPs/PTH/GCE	0.6	0.002–1.0	[54]
Electrochemical	W/ferrocyanide/[ChOx/ChEt]	10	0.05–3.0	[55]
Electrochemical	ChOx/nano-ZnO/ITI	13	0.13–10	[56]
Electrochemical	ChOx/CS-SnO <sub>2</sub> /ITO	130	0.26–10	[57]
Electrochemical	Nafion/ChOx-Ppy/PB/SAM/Pt	12	0.05–3.0	[58]
Electrochemical	ZnO@ZnS/ChOx	400	0.4–4.0	[59]
Fluorescence	Curcumin-COL-SiO <sub>2</sub> NP	2 <sup>a</sup>	0.002–10	Present work

<sup>a</sup> Minimum concentration that could change the fluorescence signal of NHPs.

**Table 2**

Recovery of synthetic samples of cholesterol using present method.

Sl. No.	Concentration of Cholesterol Taken in $\text{mmol L}^{-1}$	Concentration of Cholesterol Obtained in $\text{mmol L}^{-1}$	% of Recovery
1	0.0200	0.022 ± 2.3	110
2	0.10	0.109 ± 2.1	109
3	1.0	1.13 ± 2.2	113
4	7.0	7.16 ± 1.9	102

estimation that could detect till  $10 \mu\text{mol L}^{-1}$ . Most of the fluorescence probe based cholesterol sensors reported [23,48–50] using enzymatic reaction or non-enzymatic techniques are focused in lower detection limit and linear dynamic ranges are in  $0.0003$ – $100 \mu\text{mol L}^{-1}$  (see

Table 1), which is not of general biomedical diagnosis significance.

On the other hand, electrochemical methods reported are in different concentration ranges [19,47–60] and many of them suffer due to limited linear dynamic range and apply enzymatic reaction as summarized in Table 1. The best electrochemical method using enzymatic reaction has been reported by Solanki et al. [57] using nanostructured ZnO with a linear dynamic range  $0.13$ – $10 \text{mmol L}^{-1}$  with a detection limit of  $13 \mu\text{mol L}^{-1}$ . The present fluorescence method has a linear dynamic range  $0.002$ – $10 \text{mmol L}^{-1}$ , which shows a wider linear dynamic range than the reported one [47–60]. Nevertheless, the present method is not expected to reach lowest detection limit of the methods applied in low concentration ranges (in  $\text{nmol L}^{-1}$  concentration) due to its applicability in higher concentration ranges. For validation, synthetic samples of cholesterol were prepared and the concentrations were estimated using calibration curve obtained from

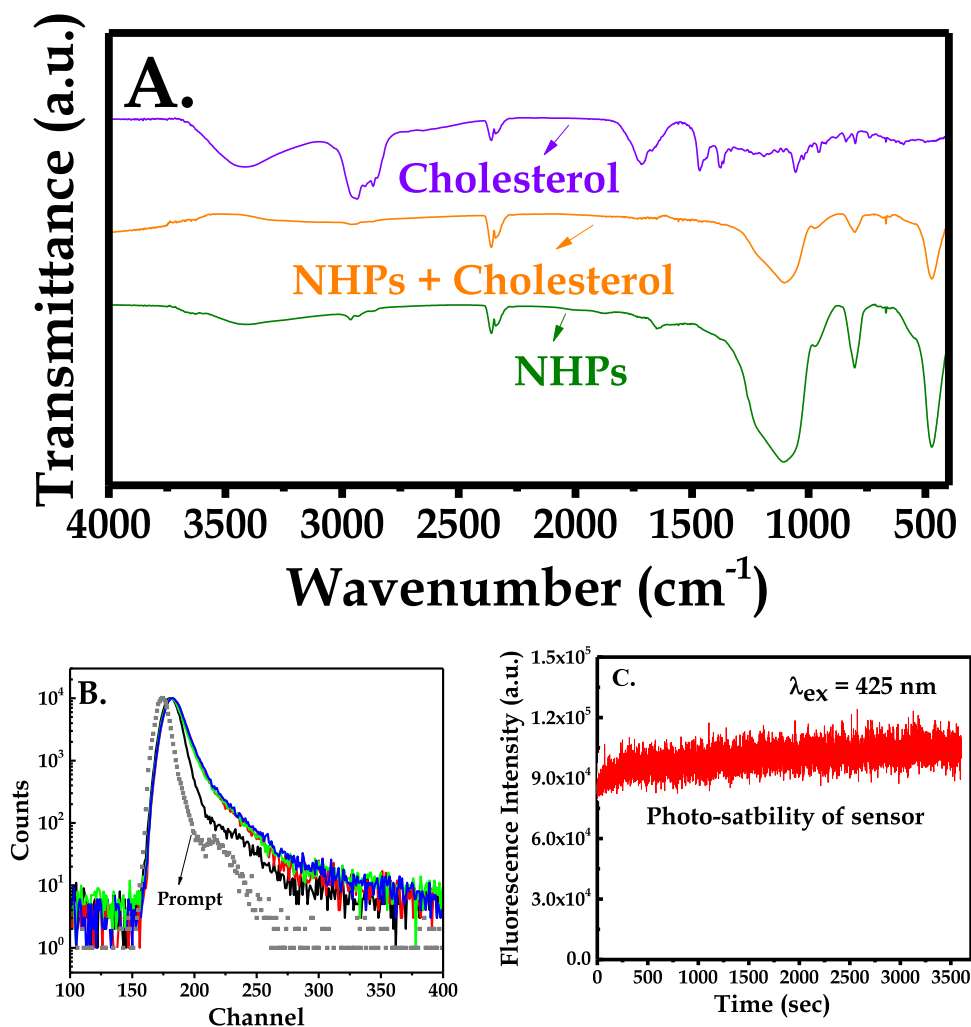


**Fig. 7.** (A) FT-IR spectra of cholesterol, NHPs and mixture of NHPs and cholesterol; (B) Excited state lifetime profile of NHPs in the absence and presence of different concentration of cholesterol; (C) Photostability of NHPs at excitation wavelength 425 nm.

this developed method. The obtained results in the form of percentage of recovery (% of recovery) as summarized in Table 2 were within 10%, which is quite acceptable.

### 3.8. Binding study and photostability of probe

The association constant of cholesterol with NHPs was estimated using the following equation [61]:

$$\log \left[ \frac{(F - F_0)}{F_0} \right] = \log(K) + n \log[\text{cholesterol}]$$

where  $K$  and  $n$  are the binding constant and the number of binding sites, respectively.  $F$  and  $F_0$  are the fluorescence intensity of NHPs at excitation wavelength 425 nm and emission wavelength 500 nm in the presence and absence of cholesterol. The association constant of cholesterol with NHPs was estimated as  $K = 6.60 \times 10^3$  liter/mol<sup>-1</sup> and number of binding sites  $n = 0.8$ , which is close to 1 as obtained from the graph in Fig. 6C. The number of binding sites qualitatively suggest not all the curcumin molecules present in NHPs is bound to cholesterol. Since NHPs are much bigger in size compared to size of cholesterol, the possibility of more than one cholesterol molecule binding to NHPs could not be ruled out. It is also important to note that one NHP has multiple numbers of curcumin units and the present  $n$  values might be because of binding between cholesterol and curcumin.

The FT-IR spectrum (see Fig. 7A) at  $\sim 3430$  cm<sup>-1</sup> for free hydroxyl group of cholesterol [62] and bands at  $\sim 3650$  cm<sup>-1</sup> and at  $\sim 3425$  cm<sup>-1</sup>

of NHPs were not clearly identified in the mixture of cholesterol and NHPs. Similarly, band at  $\sim 2948$  cm<sup>-1</sup> and  $\sim 2870$  cm<sup>-1</sup> due to C-H bond of methyl group of cholesterol was not pronounced in the mixture of cholesterol and NHPs. The band at  $\sim 1108$  cm<sup>-1</sup> due to SiO<sub>2</sub> vibration in NHPs shifted to  $\sim 1100$  cm<sup>-1</sup> in the mixture of NHPs and cholesterol. These FT-IR results suggest there is some kind of ground state electrostatic interaction through the free hydroxyl group of cholesterol along with hydrophobic interaction between NHPs and cholesterol. However, the fluorescence lifetime decay profile for NHPs in the absence and presence of cholesterol in water is shown in Fig. 7B. As can be seen the excited state lifetime of NHPs increased in the presence of cholesterol compared to in the absence of cholesterol but increase in cholesterol concentration did not influence lifetime profile remarkably. The variation of excited state lifetime profile in the presence of cholesterol does not rule out an excited state interaction between cholesterol and NHPs. The photostability of NHPs in buffer solution is illustrated in Fig. 7C. When excited at 425 nm the fluorescence intensity of NHPs within one hour did not get bleach remarkably indicating the current sensor is quite stable during measurement time.

## 4. Conclusion

Curcumin appreciably partitioned into polyelectrolyte form of COL and the association of curcumin with COL in polyelectrolyte form was found to be strong. It was found that in the presence of SiO<sub>2</sub> NP, COL

integrated with curcumin self-assembled to form nano hybrid particles. Size of these particles was in the ranges 25–35 nm with SiO<sub>2</sub> NP as its core and COL-curcumin as its outer layer having thickness of 4–8 nm. However, due to hydrophobic nature of outer layer, these NHPs aggregated in aqueous media to form large spherical structure in the ranges 1–3 μm, which could be broken down after dilution and sonication. The fluorescence spectrum of NHPs was found to be red shifted compared to free curcumin due to inner filter effect and/or homo-FRET between curcumin molecules present on the surface of individual nano hybrid particle. Although fluorescence intensity of free curcumin was substantially suppressed by Hg<sup>2+</sup>/Cu<sup>2+</sup> ions due to chelation through keto-enol form, Hg<sup>2+</sup>/Cu<sup>2+</sup> ion did affect fluorescence of NHPs, which could boost by improving analytical selectivity. The fluorescence intensity of NHPs was extraordinarily increased in the presence of cholesterol and was unaffected by ascorbic acid, uric acid, glucose and other interfering substances, thus, the present method ascertains that both the analytical selectivity and sensitivity during cholesterol estimation can be further uplifted by NHPs integrated with curcumin compare to free curcumin. The interaction between cholesterol and NHPs was found to be a combination of ground state electrostatic interaction through the free hydroxyl group of cholesterol along with hydrophobic interaction between NHPs and cholesterol and excited state interaction. The proposed method showed a wider linear dynamic range and better than most of reported method using enzymatic reaction. The NHPs were found to be photo-stable, simple, quick and cost-effective, which opens the door to develop novel analytical technique for targeted species using nano hybrid structure without using enzymatic reaction, and to tune analytical specificity, selectivity and sensitivity of probe molecule. In addition, present method could be integrated in future with emerging ordinary smart phone based optics for easy and fast detection of cholesterol at the site.

## Acknowledgement

Financial support provided by American University of Beirut, Lebanon through URB, Kamal A. Shair Research Fund as well as Kamal A. Shair Central Research Science Laboratory (KAS CRSL) facilities to carry out this work is greatly acknowledged.

## Appendix A. Supporting information

Supplementary data associated with this article can be found in the online version at doi:10.1016/j.talanta.2017.03.070.

## References

- M.R. Aguilar, J.S. Román, *Smart Polymers and their Applications*, 1st ed., Woodhead Publishing, Cambridge, U.K., 2014.
- S.N. Shtykov, T.Y. Rusanova, *Nanomaterials and nanotechnologies in chemical and biochemical sensors: capabilities and applications*, *Russ. J. Gen. Chem.* 78 (2008) 2521–2531.
- A. Sassolas, B.D. Leca-Bouvier, L.J. Blum, *DNA biosensors and microarrays*, *Chem. Rev.* 108 (2008) 109–139.
- K. Akiyoshi, S. Deguchi, N. Moriguchi, S. Yamaguchi, J. Sunamoto, *Self-aggregates of hydrophobized polysaccharides in water*, *Form. Charact. Nanopart., Macromolec.* 26 (1993) 3062–3068.
- J.W. Oha, D.I. Lee, J.M. Park, *Biopolymer-based microgels/nanogels for drug delivery applications*, *Prog. Polym. Sci.* 34 (2009) 1261–1282.
- B.H. Morrow, G.F. Payne, J. Shen, *pH-responsive self-assembly of polysaccharide through a rugged energy landscape*, *J. Am. Chem. Soc.* 137 (2015) 13024–13030.
- W. Suginta, P. Khunkaewla, A. Schulte, *Electrochemical biosensor applications of polysaccharides chitin and chitosan*, *Chem. Rev.* 113 (2013) 5458–5479.
- A.D. Martino, M. Sittinger, M.V. Risbud, *Chitosan: a versatile biopolymer for orthopaedic tissue-engineering*, *Biomater* 26 (2005) 5983–5990.
- P.F. Churchill, T. Kimura, *Topological studies of cytochromes P450<sub>acc</sub> and P450<sub>118</sub> in bovine adrenocortical inner mitochondrial membranes*, *J. Biol. Chem.* 254 (1979) 10443–10448.
- D. Sadava, D.M. Hillis, H.C. Heller, M.R. Berenbaum, *Life: The Science of Biology*, 9th ed., Freeman, San Francisco, 2011, pp. 105–114.
- K. Podar, K.C. Anderson, *Caveolin-1 as a potential new therapeutic target in multiple myeloma*, *Cancer Lett.* 233 (2006) 10–15.
- J.L. Goldstein, M.S. Brown, *Regulation of the mevalonate pathway*, *Nature* 343 (1990) 425–430.
- E. Ikonen, *Cellular cholesterol trafficking and compartmentalization*, *Nat. Rev. Mol. Cell Biol.* 9 (2008) 125–138.
- G. Yuan, J. Wang, R.A. Hegele, *Heterozygous familial hypercholesterolemia: an underrecognized cause of early cardiovascular disease*, *Can. Med. Assoc. J.* 174 (2006) 1124–1129.
- M. Sjögren, K. Blennow, *The link between cholesterol and Alzheimer's disease*, *World J. Biol. Psychiatry* 6 (2005) 85–97.
- S.B. Kritchevsky, D. Kritchevsky, *Serum cholesterol and cancer risk: an epidemiologic perspective*, *Annu. Rev. Nutr.* 12 (1992) 391–416.
- M.J. Pencina, A.M. Navar-Boggan, R.B. Sr. D'Agostino, K. Williams, B. Neely, A.D. Sniderman, E.D. Peterson, *Application of new cholesterol guidelines to a population-based sample*, *New Engl. J. Med.* 370 (2014) 1422–1431.
- D. Saraiva, R. Semedo, C. Mda Castilho, J.M. Silva, F. Ramos, *Selection of the derivatization reagent—the case of human blood cholesterol, its precursors and phyosterols GC–MS analyses*, *J. Chromatogr. B* 879 (2011) 3806–3811.
- X. Tan, M. Li, P. Cai, L. Luo, X. Zou, *An amperometric cholesterol biosensor based on multiwalled carbon nanotubes and organically modified sol-gel/chitosan hybrid composite film*, *Anal. Biochem.* 337 (2005) 111–120.
- A.K. Basu, P. Chattopadhyay, U. Roychoudhuri, R. Chakraborty, *Development of cholesterol biosensor on immobilized cholesterol esterase and cholesterol oxidase on oxygen electrode for the determination of total cholesterol in food samples*, *Bioelectrochemistry* 70 (2007) 375–379.
- S. Dong, Q. Deng, G. Cheng, *Cholesterol sensor based on electrodeposition of catalytic palladium particles*, *Anal. Chim. Acta* 279 (1993) 235–240.
- L. Zhu, L. Xu, L. Tan, H. Tan, S. Yang, S. Yao, *Direct electrochemistry of cholesterol oxidase immobilized on gold nanoparticles-decorated multiwalled carbon nanotubes and cholesterol sensing*, *Talanta* 106 (2013) 192–199.
- N. Li, A. Than, X. Wang, S. Xu, L. Sun, H. Duan, C. Xu, P. Chen, *Ultrasensitive profiling of metabolites using tyramine-functionalized graphene quantum dots*, *ACS Nano* 10 (2016) 3622–3629.
- K.-E. Kim, T.G. Kim, Y.-M. Sung, *Fluorescent cholesterol sensing using enzyme-modified CdSe/ZnS quantum dots*, *J. Nanopart. Res.* 14 (2012) (1179–1179).
- Y. Cheng, P. Jiang, S. Lin, Y. Li, X. Dong, *An imprinted fluorescent chemosensor prepared using dansyl-modified β-cyclodextrin as the functional monomer for sensing of cholesterol with tailor-made selectivity*, *Sens. Actuatur. B: Chem.* 193 (2014) 838–843.
- M.E. Egan, M. Pearson, S.A. Weiner, V. Rajendran, D. Rubin, J. Glöckner-Pagel, S. Canny, K. Du, G.L. Lukacs, M.J. Caplan, *Curcumin, A major constituent of turmeric, corrects cystic fibrosis defects*, *Science* (304) (2004) 600–602.
- E. El Khoury, D. Patra, *Ionic liquid expedites partition of curcumin into solid gel phase but discourages partition into liquid crystalline phase of 1,2-dimyristoyl-sn-glycero-3-phosphocholine liposomes*, *J. Phys. Chem. B* 117 (2013) 9699–9708.
- M. Mouslmani, K.H. Bouhadir, D. Patra, *Poly (9-(2-diallylaminoethyl)denine HCl-Co-sulfur dioxide) deposited on silica nanoparticles constructs hierarchically ordered nanocapsules: curcumin conjugated nanocapsules as a novel strategy to amplify guanine selectivity among nucleobases*, *Biosens. Bioelectro.* 68 (2015) 181–188.
- R.N. Moussawi, D. Patra, *Synthesis of Au nanorods through prereduction with curcumin: preferential enhancement of Au nanorod formation prepared from CTAB-capped over citrate-capped Au seeds*, *J. Phys. Chem. C* 119 (2015) 19458–19468.
- I. Alwi, T. Santoso, S. Suyono, B. Sutrisna, F.D. Suyatna, S.B. Kresno, S. Ernie, *The effect of curcumin on lipid level in patient with acute coronary syndrome*, *Acta Med. Indones.* 40 (2008) 201–210.
- S.P. Davis, *Chitosan: Manufacture, Properties, and Usage*, Nova Science Publishers, Inc, Hauppauge: New York, U.S.A., 2011.
- M. Chebl, M.G. Abiad, Z. Moussa, D. Patra, *Two modes of associations of curcumin with pre- and nano-aggregated chitosan oligosaccharide lactate: ionic strength and hydrophobic bile salt modulate partition of drug and self-assembly process*, *J. Phys. Chem. C* 120 (2016) 11210–11224.
- Z. Huang, R.P. Haugland, *Partition coefficients of fluorescent probes with phospholipid membranes*, *Biochem. Biophys. Res. Comm.* 181 (1991) 166–171.
- M. Mouslmani, D. Patra, *Revoking excited state intra-molecular hydrogen transfer by size dependent tailored made hierarchically ordered nanocapsules*, *RSC Adv.* 4 (2014) 8317–8320.
- D. Patra, F. Sleem, *A new method for pH triggered curcumin release by applying poly (L-lysine) mediated nanoparticle-congregation*, *Anal. Chim. Acta* 795 (2013) 60–68.
- D. Patra, A.J. Amali, R.K. Rana, *Preparation and photophysics of HPTS based nanoparticle-assembled microcapsules*, *J. Mater. Chem.* 19 (2009) 4017–4021.
- S.-M. Lai, A.J. Yang, W.-C. Chen, J.-F. Hsiao, *The properties and preparation of chitosan/silica hybrid using sol-gel process*, *Polym.-Plast. Tech. Engine.* 45 (2006) 997–1003.
- W. Abdelwahed, G. Degobert, S. Stainmesse, H. Fessi, *Freeze-drying of nanoparticles: formulation, process and storage consideration*, *Adv. Drug. Del. Rev.* 58 (2006) 1688–1713.
- J. Shaikh, D.D. Ankola, V. Beniwal, D. Singh, M.N. Kumar, *Nanoparticle encapsulation improves oral bioavailability of curcumin by at least 9-fold when compared to curcumin administered with piperine and absorption enhancer*, *Eur. J. Pharm. Sci.* 37 (2009) 223–230.
- F. Zsila, Z. Bikádi, M. Simonyi, *Molecular basis of the Cotton effects induced by the binding of curcumin to human serum albumin*, *Tetrahedron.: Asymmetry* 14 (2003) 2433–2444.
- L. Shen, H.-Y. Zhang, H.-F. Ji, *Successful application of TD-DFT in transient*

- absorption spectra assignment, *Org. Lett.* 7 (2005) 243–246.
- [42] J.R. Lakowicz, *Principles of Fluorescence Spectroscopy*, Kluwer Academic, Plenum Publishers, New York, USA, 1999.
- [43] S.-H. Kim, S. -Y. Gwon, S.M. Burkinshaw, Y.-A. Son, The photo- and electro-physical properties of curcumin in aqueous solution, *Spectrochim. Acta Part A* 76 (2010) 384–387.
- [44] X.-Z. Zhao, T. Jiang, L. Wang, H. Yang, S. Zhang, P. Zhou, Interaction of curcumin with Zn (II) and Cu (II) ions based on experiment and theoretical calculation, *J. Mol. Struct.* 984 (2010) 316–325.
- [45] D. Patra, D. Ahmadi, R. Aridi, Study on interaction of bile salts with curcumin and curcumin embedded in dipalmitoyl-sn-glycero-3-phosphocholine liposome, *Colloids Surf. B: Biointerfaces* 110 (2013) 296–304.
- [46] R. Qu, C. Sun, C. Ji, C. Wang, H. Chen, Y. Niu, C. Liang, Q. Song, Preparation and metal-binding behaviour of chitosan functionalized by ester- and amino-terminated hyperbranched polyamidoamine polymers, *Carbohydr. Res.* 343 (2008) 267–273.
- [47] H.-C. Chang, J.-A. Ho, Gold nanocluster-assisted fluorescent detection for hydrogen peroxide and cholesterol based on the inner filter effect of gold nanoparticles, *Anal. Chem.* 87 (2015) 10362–10367.
- [48] D.M. Amundson, M. Zhou, Fluorometric method for the enzymatic determination of cholesterol, *J. Biochem. Biophys. Methods* 38 (1999) 43–52.
- [49] N. Zhang, Y. Liu, L. Tong, K. Xu, L. Zhuo, B. Tang, A novel assembly of Au NPs- $\beta$ -CDs-FL for the fluorescent probing of cholesterol and its application in blood serum, *Analyst* 133 (2008) 1176–1181.
- [50] Y. Ding, H. Zhu, X. Zhang, J. Gao, E.S. Abdel-Halim, L. Jiang, J.-J. Zhu, An upconversion nanocomposite for fluorescence resonance energy transfer based cholesterol-sensing in human serum, *Nanoscale* 6 (2014) 14792–14798.
- [51] S. Komathi, N. Muthichamy, K.P. Lee, A.I. Gopalan, Fabrication of a novel dual mode cholesterol biosensor using titanium dioxide nanowire bridged 3D grapheme nanostacks, *Biosens. Bioelectron.* 84 (2016) 64–71.
- [52] T. Yao, K. Takashima, Amperometric biosensor with a composite membrane of sol-gel derived enzyme film and electrochemically generated poly (1,2-diaminobenzene) film, *Biosens. Bioelectron.* 13 (1998) 67–73.
- [53] B.C. Ozer, H. Ozyoruk, S.S. Celebi, A. Yildiz, Amperometric enzyme electrode for free cholesterol determination prepared with cholesterol oxidase immobilized in poly (vinylferrocene) film, *Enzyme Microb. Technol.* 40 (2007) 262–265.
- [54] Y. Li, H. Bai, Q. Liu, J. Bao, M. Han, Z. Dai, A nonenzymatic cholesterol sensor constructed using porous tubular silver nanoparticles, *Biosens. Bioelectron.* 25 (2010) 2356–2360.
- [55] Q. Huang, Y. An, L. Tang, X. Jiang, H. Chen, W. Bi, Z. Wang, W. Zhang, A dual enzymatic-biosensor for simultaneous determination of glucose and cholesterol in serum and peritoneal macrophages of diabetic mice: evaluation of the diabetes-accelerated atherosclerosis risk, *Anal. Chim. Acta* 707 (2011) 135–141.
- [56] M. Situmorang, P.W. Alexander, D.B. Hibbert, Flow injection potentiometry for enzymatic assay of cholesterol with a tungsten electrode sensor, *Talanta* 49 (1999) 639–649.
- [57] P.R. Solanki, P.R. Kaushik, A.A. Ansari, G. Sumana, B.D. Malhotra, Nanostructured zinc oxide platform for cholesterol sensor, *Appl. Phys. Lett.* 94 (2009) 143901.
- [58] A.A. Ansari, A. Kaushik, P.R. Solanki, B.D. Malhotra, Electrochemical cholesterol sensor based on tin oxide-chitosan nanobiocomposite film, *Electroanalysis* 21 (2009) 965–972.
- [59] J.C. Vidal, J. Espuelas, E. Garcia-Ruiz, J.R. Castillo, Amperometric cholesterol biosensors based on the electropolymerization of pyrrole and the electrocatalytic effect of Prussian-blue layers helped with self-assembled monolayers, *Talanta* 64 (2004) 655–664.
- [60] A.K. Giri, C. Chran, S.C. Ghosh, V.K. Shahi, A.B. Panda, Phase and composition selective superior cholesterol sensing performance of ZnO@ZnS nano-heterostructure and ZnS nanotubes, *Sens. Actuators B: Chem.* 229 (2016) 14–24.
- [61] K.A. Connors, *Binding Constants. the Measurements of Molecular Complex Stability*, Wiley, New York, USA, 1978.
- [62] M.M. Paradkar, J. Irudayaraj, Determination of cholesterol in dairy products using infrared techniques: 1. FTIR spectroscopy, *Int. J. Dairy Technol.* 55 (2002) 127–132.